THE JOURNAL OF PHYSICAL CHEMISTRY B

Article

pubs.acs.org/JPCB

Kinetic Analysis of Quasi-One-Dimensional Growth of Polymer Lamellar Crystals in Dilute Solutions

Yujie Zhou and Wenbing Hu*

Department of Polymer Science and Engineering, State Key Laboratory of Coordination Chemistry, School of Chemistry and Chemical Engineering, Nanjing University, 210093 Nanjing, China

ABSTRACT: Flexible polymers are featured with two-dimensional growth of metastable chain-folded lamellar crystals in quiescent dilute solutions. Recently, a massive cylindrical micelle with quasi-one-dimensional (quasi-1D) growth driven by confined crystallization of diblock copolymers in dilute solutions raised a new challenge. We performed dynamic Monte Carlo simulations to investigate the kinetics of quasi-1D growth of lamellar crystals in two typical cases of dilute but not very dilute polymer solutions. We found that in both cases the growth kinetics is dominated by the surface-nucleation-controlled mechanism. Moreover, in the first case corresponding to few and small crystals grown under almost constant polymer concentrations in the huge bulk of solutions, the driving-force term in the kinetic equation dominates a linear concentration dependence of crystal growth rates in the high-concentration region, and the nucleation-barrier term dominates their nonlinear deviation in the low-concentration region. In the second case corresponding to massive crystals grown under depleting polymer concentrations in a limited volume of solutions, the crystal growth rates decay with time, but at the early stage, they follow exactly with the linear-concentration-dependent growth rates of the first case. Therefore, the growth size at the early stage of the second case can be described as an exponential-decay function of time, which provides a theoretical model to the data analysis of corresponding experimental observations.

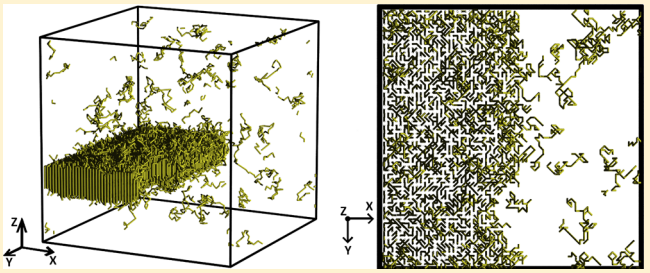

I. INTRODUCTION

Solution crystal growth is an important issue in chemical, biological, geological, pharmaceutical, and materials sciences.[1,2] On this issue, chain-like macromolecules exhibit some specific crystallization behaviors.[3] For instance, polymers intend to fold up and then form metastable lamellar single crystals in quiescent dilute solutions.[4] Over the past 50 years, a lot of theoretical and experimental efforts have been put into the study of the growth kinetics of polymer lamellar crystals in solutions.[5−10] Recently, massive self-seeded crystallization-driven self-assembly of poly(isoprene-*b*-ferrocenyldimethylsilane) diblock copolymers in dilute solutions has raised new attention,[11,12] which exhibits quasi-1D cylindrical growth with other two dimensions restricted by the surrounding non-crystallizable blocks. In such a typical case, polymers deplete in the solution space upon crystal growth, and the crystal growth rates decrease with time evolution. So far, two basic theoretical mechanisms dominating the kinetics of crystal growth in dilute solutions, i.e., the limited long-distance diffusion and the surface-nucleation barrier, both predict the decay of crystal growth rates upon the decrease of polymer concentrations,[3] demanding further identification of the right one here.

The conventional case to study the crystallization kinetics in dilute polymer solutions is few and small single crystals grown in a huge solution reservoir, with polymer concentration (C_0) almost constant upon crystal growth. In this case, if the surface nucleation (the deposition of solute molecules onto the crystal surface typically via secondary crystal nucleation at a low supercooling $\Delta T = T_m - T$, where T_m is the equilibrium melting point and T the crystallization temperature) dominates the growth kinetics, the linear crystal growth rates (G) keep constant over the time evolution and meanwhile their concentration dependence can be empirically expressed as[1−3]

$$G \propto C_0^{\alpha} \tag{1}$$

The exponent α varies from 0.2 to 2 under various circumstances reported in the literature, and appears smaller at higher molecular weights and lower crystallization temperatures.[13−16] Keller and Pedemonte suggested that a weak concentration dependence of growth rates ($\alpha < 1$) implies the cilia competing with free polymers in the process of surface nucleation,[6] while the strong dependence ($\alpha > 1$) implies more than one chain is involved in the nucleation process.[13] Toda and Kiho studied the concentration dependence of the nucleation rate and the velocity of step propagation of polyethylene, and concluded that the volume diffusion rate influences the value of α only at extremely diluted solutions ($<10^{-4}$ wt %).[17] If the lamellar crystal growth of polymer chains is dominated by surface nucleation, the linear crystal growth rates can be regarded as the net result of competition between

Received: December 3, 2012
Revised: February 17, 2013
Published: February 18, 2013

 © 2013 American Chemical Society

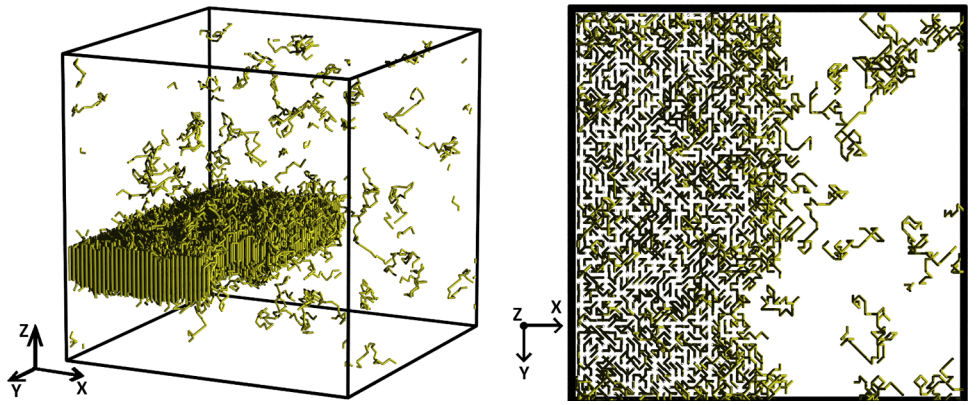

Figure 1. Snapshots from two view angles on a dilute 32-mer solution with the volume fraction 0.0097 in a 64^3 cubic lattice after being crystallized at $T = 3.4$ for 10^7 cycles, to demonstrate one-dimensional growth of a single lamellar polymer crystal along the X-axis. Polymer bonds are drawn in yellow cylinders. The crystal seed with the size $1 \times 64 \times 8$ spans over periodic boundary conditions along the Y-axis at $X = 1$, and the crystalline stems are aligned along the Z-axis at $Z = 16$.

crystal growth and melting at the lateral growth front, as given by[18,19]

$$G \approx G_{\text{barrier}}(l - l_{\text{min}})\frac{b^2\Delta f}{kT} \tag{2}$$

where $l - l_{\text{min}}$ is the excess length of crystalline stems (lamellar thickness) beyond the minimum stable length, b is the thickness of crystalline stems, Δf is the free energy change of crystallization per unit volume, which is roughly proportional to the supercooling $\Delta T = T_{\text{m}} - T$, k is the Boltzmann's constant, and the barrier term for surface nucleation is[3]

$$G_{\text{barrier}} \propto \exp\left(-\frac{4b\sigma\sigma_{\text{e}}}{kT\Delta f}\right) \tag{3}$$

Here, σ and σ_{e} are the surface energies on the lateral surface and on the fold-end surface, respectively. In eq 2, the terms other than the barrier term belong to the driving-force term. In dilute solutions, the supercooling ΔT is presumably proportional to the supersaturation $C_0 - C_{\text{m}}$, where C_{m} is the equilibrium polymer concentration at the crystallization temperature, and is often negligible due to its relatively small value. If the crystal growth rates are dominated by the driving-force term, the exponent is $\alpha = 1$; if they are dominated by the barrier term, they will be more sensitive to the change of polymer concentrations, and the exponent α appears much larger. How the growth kinetics in the constant-concentration case could be connected to that in the depleting-concentration case is worthy of further investigation as well.

Molecular simulations provide a molecular-level approach to investigate crystal growth in polymer solutions.[20] However, crystal growth in dilute polymer solutions is normally orders of magnitude slower than that in the concentrated solutions and the melt phase.[13] The major difficulty of simulations arises from the longer-term and larger-size scales to match for the experimental reality. In this sense, the highly efficient Monte Carlo simulations of coarse-grained polymer models show their privileges over molecular dynamics simulations that include explicit solvent molecules.[21] Muthukumar et al. recently performed Monte Carlo simulations of an "anisotropic aggregation" model in which each lattice unit represented a single folded chain in a dilute solution.[22] This model captured some kinetic features in the morphology evolution of polymer single crystals, but it did not study the kinetics of quasi-1D crystal growth, especially under the effect of chain lengths. In this paper, we performed dynamic Monte Carlo simulations of a lattice polymer-chain model to focus on the linear rates of quasi-1D crystal growth in dilute solutions. The model is efficient enough to observe the crystal growth process in a wide time window and meanwhile does not lose the information about chain conformation and orientations. The effectiveness of this model has been illustrated with our previous investigations on the growth of chain-folded lamellar crystals of polymers in semidilute solutions.[10] We set up quasi-1D lamellar crystal growth with its lateral dimension spreading over the periodic boundary of a small lattice box. We separated our observations into two growth cases: the first one feeds polymers into the solution space upon crystal growth to maintain constant polymer concentrations, while the second one depletes polymers in the solution space upon crystal growth without any feeding. In the first case, we observed a linear relationship between crystal growth rates and polymer concentrations, while, in the second case, the early stage growth rates decrease with time but appear consistent with the growth rates in the linear-concentration-dependent region of the first case. The linear relationship implies an exponential decay of the linear growth size with time evolution, which provides a theoretical model to the data analysis of real parallel systems.

After the Introduction section, we introduce the simulation methods followed with the simulation results separated into two cases. The paper ends with a summary of our conclusions.

II. SIMULATION METHODS

We set up the polymer solution system in a $64 \times 64 \times 64$-sized cubic lattice box with periodic boundary conditions. Each chain unit occupied one lattice site, and two consecutive units formed a bond connection along the chain. Polymers of 16, 32, 64, and 256 units long were investigated. Chains shorter than 16 could only form extended chains in the lamellar crystals, while those longer than 256 units may interact with their own images through periodic boundaries of the lattice box.

The chains performed trial moves with a microrelaxation mode of single-site jumping and local sliding diffusion.[23] The moves were sampled by the conventional Metropolis algorithm: trial moves were rejected if they caused hard-core overlaps or bond crossing; otherwise, they were accepted with a probability equal to the minimum $\min(1, \exp[-\Delta E/(kT)])$, where ΔE was

dx.doi.org/10.1021/jp311889n | J. Phys. Chem. B 2013, 117, 3047−3053

the net energy change of the system after each trial move. The total energy E could be expressed as

$$E = \Sigma\varepsilon_p + \Sigma\varepsilon_c + \Sigma\varepsilon_b \quad (4)$$

where the term ε_p was an attractive energy between two parallel-packed bonds (each bond contains 26 "neighbors" that sit around it along all the axes and diagonals in a 3 × 3 cube, two of which are often connected along the chain; thus, only 24 of them could be parallel to the center bond and contributed to ε_p), the term ε_c was an energetic penalty for a gauche conformation (two consecutive bonds along a chain but not aligned in a straight line), and the term ε_b denoted the mixing interaction of monomer−solvent pairs. For simplicity, the solvent was assumed to be athermal ($\varepsilon_b = 0$), the interaction ratio was fixed at $\varepsilon_p/\varepsilon_c = 1$, and the reduced temperature kT/ε_c was used as the system temperature (denoted as T below). The total amount of trial moves for one average attempt over all the monomers was defined as one cycle, serving as the time unit in our simulations.

To initiate quasi-1D lamellar crystal growth, a seed of crystal template consisting of one preset array of regularly folded chains with the sizes of 1 × 64 × 8 was set at $X = 1$ and $Z = 32$, which spanned along the Y-axis over the periodic boundary (see Figure 1). We let crystal grow along the X-axis (rather than both sides with $-X$ direction) by setting the interaction ε_p of polymer chains only on the $+X$ side of those bonds in the seed. The bond was counted as crystalline when more than 15 of its 24 neighboring bonds were parallel with it. The chain was counted as crystallized when more than half of its bonds were crystalline. The linear size of the growing crystal (L) along the X-axis was defined by the largest distance of the crystalline stems (containing at least three consecutive crystalline bonds along the Z-axis) away from the seed, after being averaged over the Y-axis. The linear growth rate (G) could thus be obtained from the derivative of L with respect to time. The volume fraction of chains (C) that were not crystallized was used to characterize the polymer concentration in the solution space. Polymer concentrations and the reduced temperatures were ranged under the considerations of the available computation time window (crystals growing slower at lower C and higher T) and of the avoidance of spontaneous primary nucleation (primary nucleation becoming faster at higher C and lower T). All reported data was averaged over several independent observations to make an error bar.

Our simulations were carried out in two separate cases. The first case maintained constant polymer volume fractions, by feeding one chain randomly into the solution space once a chain was accepted by crystal growth. The second case let polymers be depleted in the solution space upon crystal growth with a fixed total amount of chains. In this sense, the first case will eventually end crystal growth at the periodic boundary of the box, and the second case stops crystal growth at somewhere when almost all the free amorphous chains are exhausted. The crystal thickness is mainly dominated by the crystallization temperature,[3−10] which remains constant upon and even after crystal growth in dilute solutions. In this work, we will analyze the concentration dependence of the linear growth rates in two cases, and compare their kinetics of crystal growth.

III. SIMULATION RESULTS

A. Crystal Growth with Constant Polymer Concentration C_0. We first traced the time evolution of the crystal growth front at various low concentrations for a chain length of 64 at the temperature 3.1. The results are summarized in Figure 2. One can see that a good linear time dependence generally

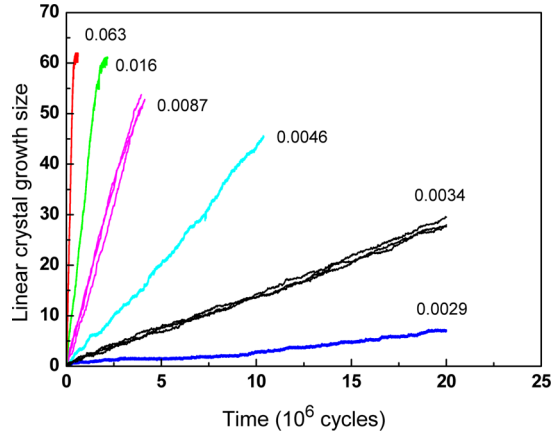

Figure 2. Time evolution of the crystal growth sizes with various polymer volume fractions C_0 kept constant and denoted nearby, for the chain length $N = 64$ and $T = 3.1$. Each curve corresponds to an individual observation in simulations.

exists in the time evolution of the linear growth sizes, and the slope gives a constant linear crystal growth rate with the reported value averaged over several independent parallel observations. The constant linear crystal growth rates exempt the diffusion-limited mechanism and suggest the surface-nucleation mechanism. We go further to analyze the concentration dependence of the linear crystal growth rates for various chain lengths and crystallization temperatures, as summarized in Figure 3.

Figure 3a−c shows the double logarithmic plots of G versus C_0 with various chain lengths at three temperatures, respectively. By comparisons of parallel curves of the same chain lengths in the three parts of the figure, one can see that the linear crystal growth rates are larger at lower temperatures, implying again a nucleation-controlled mechanism of crystal growth. A linear concentration dependence (mainly with $\alpha = 1$) occurs generally in the high-concentration region, implying the driving-force term responsible for this linear relationship in the surface-nucleation mechanism of lamellar crystal growth. The similar trends of linear relationship were also observed by Keller and Pedemonte,[13] and according to their suggestion, the linear concentration dependence might imply the intramolecular crystal nucleation, i.e., each surface nucleus evolving only one short polymer chain.[3,24] Indeed, in most cases, the crystal growth rates are insensitive to the chain lengths, as predicted well by the intramolecular nucleation model.[24]

Further evidence of nucleation-controlled growth mechanism could be obtained from the temperature dependence of crystal growth rates, in both high- and low-concentration regions, as for example, shown in Figure 4. According to eqs 2 and 3, the temperature dependence of linear crystal growth rates is mainly dominated by the secondary nucleation barrier; thus, one derives

$$\log G \propto \frac{K_g}{T\Delta T} \quad (5)$$

where K_g is called the nucleation constant. In the secondary-nucleation plot $\log G$ versus $(T\Delta T)^{-1}$, the linear relationship

dx.doi.org/10.1021/jp311889n | J. Phys. Chem. B 2013, 117, 3047−3053

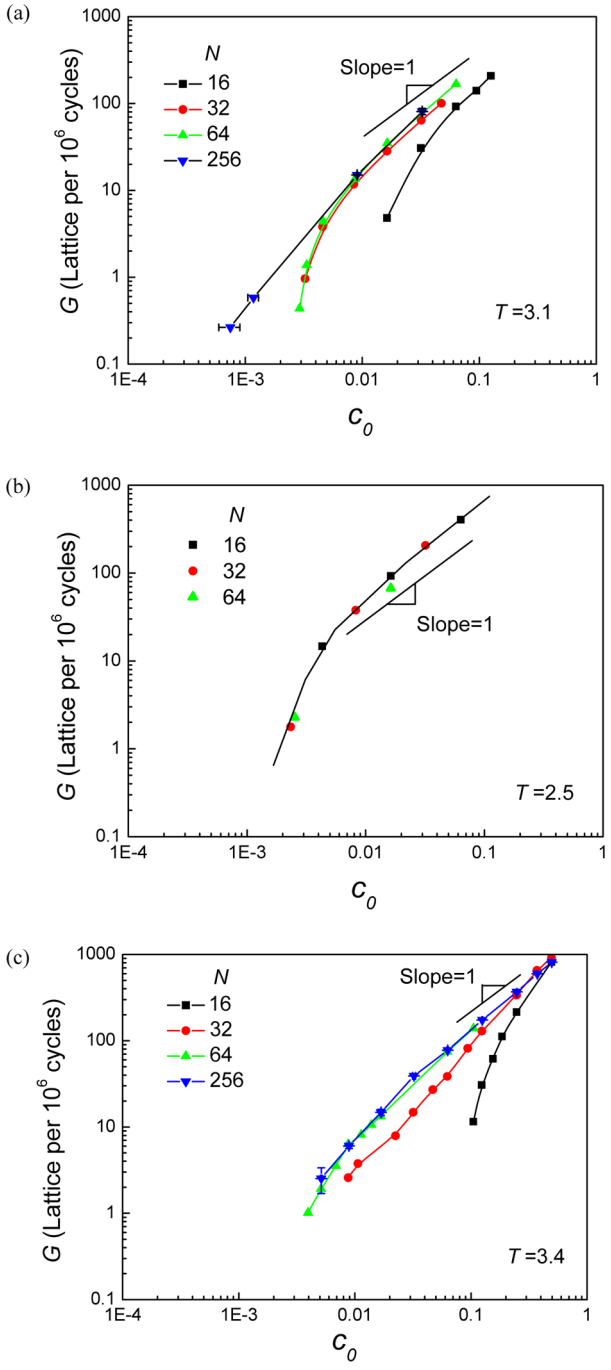

Figure 3. Double logarithmic plots of linear crystal growth rates versus polymer volume fractions on crystal growth under constant polymer concentrations for N = 16, 32, 64, and 256 at (a) T = 3.1, (b) T = 2.5, and (c) T = 3.4. The lines are drawn to guide the eyes.

has been generally applied to demonstrate the nucleation-controlled mechanism of polymer crystal growth rates.[10] In three different temperature regimes, the nucleation constants jump with their ratios 2:1:2.[10] In Figure 4a, the linear fitting gives a good linear correlation with K_g = −3.84, while, in Figure 4b, the linear fitting gives a good correlation with K_g = −1.92. The exactly half relationship of K_g values implies that the lower-shifted regime II at the low concentration shares the same growth-rate window with the regime I at the high concentration.

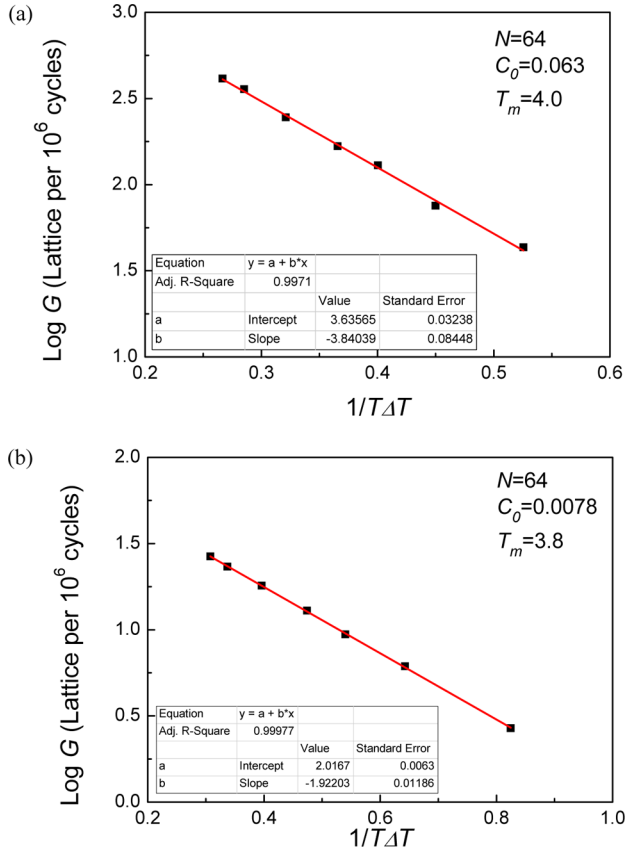

Figure 4. Secondary-nucleation plots (see eq 5) of linear crystal growth rates of 64-mers for their temperature dependences at (a) C_0 = 0.063 in the high-concentration region with the supposed T_m = 4.0 and (b) C_0 = 0.0078 in the low-concentration region with the supposed T_m = 3.8. The straight lines are the fitting lines with fitting parameters summarized in the inset tables.

In the lower concentration region in Figure 3, the nonlinear deviations of crystal growth rates from the general linear concentration dependence are related with the shortage of thermodynamic driving forces (supersaturation) due to their approaching to the equilibrium concentration C_m. The linear crystal growth rates remain constant over time evolution. Thus, the nonlinear concentration dependence of the crystal growth rates is dominated by the barrier term in eq 3, rather than by the long-distance diffusion. We have estimated the diffusion coefficient from the saturated horizontal in the time (t) evolution curve of mean-square displacement of the mass center of polymer chains divided by 6t in 64-mer homogeneous solutions at T = 3.4 without the template for crystal growth. The results are 0.00644 ± 0.00111, 0.00557 ± 0.00034, 0.00508 ± 0.00016, and 0.00411 ± 0.00012 lattice^2/cycle separately at polymer volume fractions of 0.00195, 0.0078, 0.0625, and 0.125. The diffusion coefficients appear slightly decreasing with the increase of concentrations, showing an opposite trend of the linear crystal growth rates. One more piece of evidence comes from the concentration dependence of the detachment/attachment ratios of polymers at the growth front during crystal growth. An attachment event of polymers was defined as a free polymer harvesting crystalline bonds more than half of its chain length in one cycle at the growth front; meanwhile, a detachment event of polymers was defined as an attached polymer dissolving into a free polymer in the solution space. We counted events of detachment and attachment of

dx.doi.org/10.1021/jp311889n | J. Phys. Chem. B 2013, 117, 3047−3053

polymers in each cycle during steady crystal growth, and reported their average ratios. Such a ratio reflects the failure probability of trial events for surface nucleation. The results of the ratios obtained at various concentrations are summarized in Figure 5. One can see that in the low-concentration region,

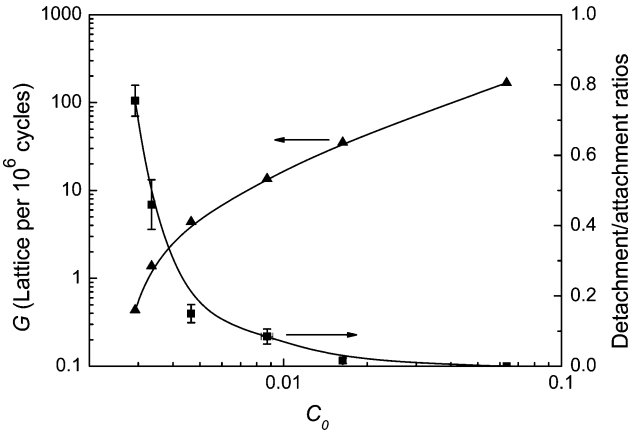

Figure 5. Detachment/attachment ratios of polymers at the growth front in comparison with the double logarithmic linear crystal growth rates versus polymer volume fractions that were maintained as constant upon crystal growth of 64-mers at T = 3.1.

once the growth rates deviate from the linear concentration dependence, the detachment/attachment ratios of polymers increase, implying higher nucleation difficulty due to the lack of supersaturation (less thermodynamic driving forces). The limited long-distance diffusion in the low-concentration region will give an opposite trend if it controls the crystal growth kinetics. In the high-concentration region, the nucleation barrier is quite low due to large supersaturation, so the driving-force term in eq 2 dominates the concentration dependence of the crystal growth rates. In conclusion, the surface-nucleation mechanism dominates the kinetics of crystal growth in our observations of the first case.

In Figure 3b, the crystal growth rates appear insensitive to the chain lengths at low temperatures, which can be assigned to the mechanism controlled by the intramolecular crystal nucleation. In Figure 3a and c, the lower shifts of linear crystal growth rates of 16-mers and 32-mers can be attributed to their relatively lower harvest of crystallinity in each event of intramolecular surface nucleation at high temperatures, due to their lesser amount of monomers in each chain, as observed in the previous simulations of cocrystallization of binary mixtures of two chain lengths (16-mers and 32-mers).[25] The higher crystallization temperatures also make surface nucleation more difficult; thus in Figure 3c, the crystal growth rates in 16-mer solutions start to deviate from the linear curves at higher concentrations, in comparison to that in 32-mer solutions.

B. Crystal Growth with the Depletion of Polymers. In the second case, the total amount of polymer chains was fixed. Polymers were depleted in the solution space upon crystal growth, which will lead to a continuous decay in the supersaturations as well as in the linear crystal growth rates. So far, it is not clear whether the decrease of crystal growth rates is dominated by the diffusion-controlled mechanism or by the surface-nucleation-controlled mechanism. Figure 6 shows the time-evolution curves of linear crystal sizes at several initial polymer concentrations for 64-mers at the temperature 3.4.

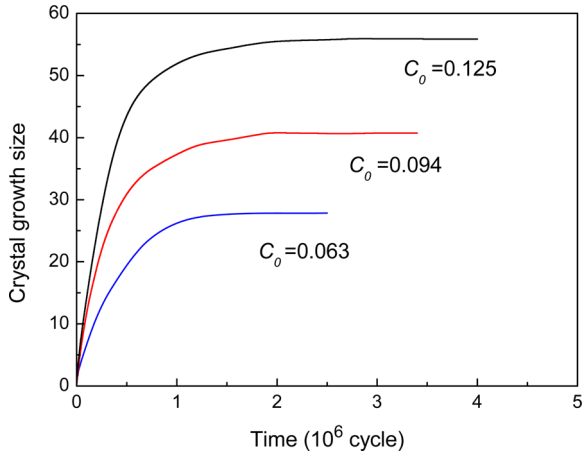

Figure 6. Time-evolution curves of the linear crystal growth sizes with a decay from various initial polymer volume fractions as denoted, for the chain length N = 64 and the temperature T = 3.4. Each curve corresponds to an individual simulation with a specific initial polymer volume fraction.

In the second case, the increase of crystal growth sizes is gradually saturated with the time evolution when polymers become exhausted in the bulk solution phase (see Figure 6). One can get the instant linear crystal growth rates G from the time derivative of the linear growth sizes L. The time evolution can also be characterized into the instant concentration (C) evolution. Thus, we can make the double logarithmic plot of G versus C and compare the results to the linear crystal growth rates obtained from the first case with parallel concentrations, as shown in Figure 7. One can clearly see that, at the early

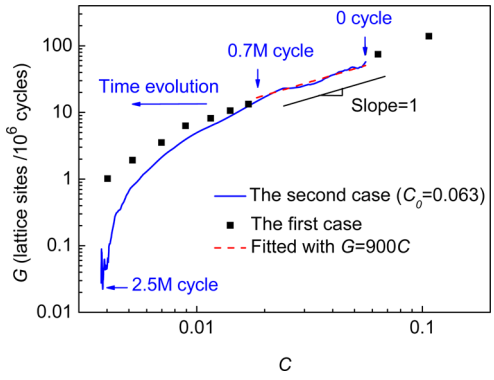

Figure 7. Comparison of double-logarithmic curves of linear crystal growth rates versus polymer volume fractions between the first and second cases for the chain length N = 64 at the temperature T = 3.4. The arrows indicate the time periods for crystal growth in the second case. A linear fitting was performed at the early stage with G = 900C. The very early short time period for reaching a steady growth was discarded.

stage, the linear crystal growth rates in the second case (the blue curve) follow exactly with those parallel results in the first case. At the later stage, the growth rates in the second case drop drastically as the system is approaching the exhausted end. The consistence of the linear crystal growth rates in the linear-concentration-dependent region (see the fitted segment) indicates that, at the early stage of the second case, the linear crystal growth rates are dominated by the surface-nucleation-controlled mechanism at the crystal growth front. The

dx.doi.org/10.1021/jp311889n | J. Phys. Chem. B 2013, 117, 3047−3053

deviation from the linear relationship at the later stage is not so significant, implying a long-term nucleation-controlled growth in the second case.

C. Data Treatment of Crystal Growth Sizes in the Second Case. For quasi-1D growth of the lamellar crystals of polymers with a fixed lamellar thickness at a specific temperature, one assumes that the linear growth sizes are proportional to the consumed amount of polymers in the second case, as given by

$$L = B(C_0 - C) \tag{6}$$

where B is a coefficient for the total volume divided by the boundary distance along the Y-axis and by the lamellar thickness (depending upon temperature) and C_0 is the initial concentration. By definition, the linear crystal size can be expressed as

$$L = \int_0^t G \, d\tau \tag{7}$$

G has a linear relationship with polymer concentrations at the early stage according to Figure 7

$$G = AC \tag{8}$$

where A is a constant, as fitted from the linear segment in Figure 7. On the basis of the equations shown above, we can get

$$B(C_0 - C) = \int_0^t AC \, d\tau \tag{9}$$

The solution of the above equation is

$$C = C_0 e^{-Dt} \tag{10}$$

where

$$D \equiv \frac{A}{B}$$

Then, we obtain the prediction of the linear growth sizes as a function of time at the early stage as

$$L = BC_0(1 - e^{-Dt}) \tag{11}$$

To obtain the coefficient B in eq 6, the plot of L versus C is fitted at the early stage (see Figure 8a). Then, we compare the fitted theoretical curve with the simulation results for L versus time t in Figure 8b. One can see that the time evolution of L can be well predicted by eq 11 with the fitting parameters at the early stage of crystal growth. One can also observe the time evolution of C (Figure 8c), which is predicted well with eq 10 at the early stage.

The lower-size deviation at the later stage of crystal growth in the second case can be attributed to the slowing down of crystal growth due to the deviation of linear concentration scaling at the low concentration region. To get a better fitting for the L-versus-t data, we choose an empirical double exponential function, anticipating that at the later stage the growth also obeys some sort of exponential-decay functions but much weaker than the early stage. The second exponential function makes partial compensation to the overestimation of the ideal extrapolation from the early stage. The curve can then get a better fitting for the overall growth process (see Figure 9). The data fitting based on the double logarithmic function has been well applied in the kinetic analysis of the quasi-1D micelle growth in dilute solutions of diblock copolymers.[26]

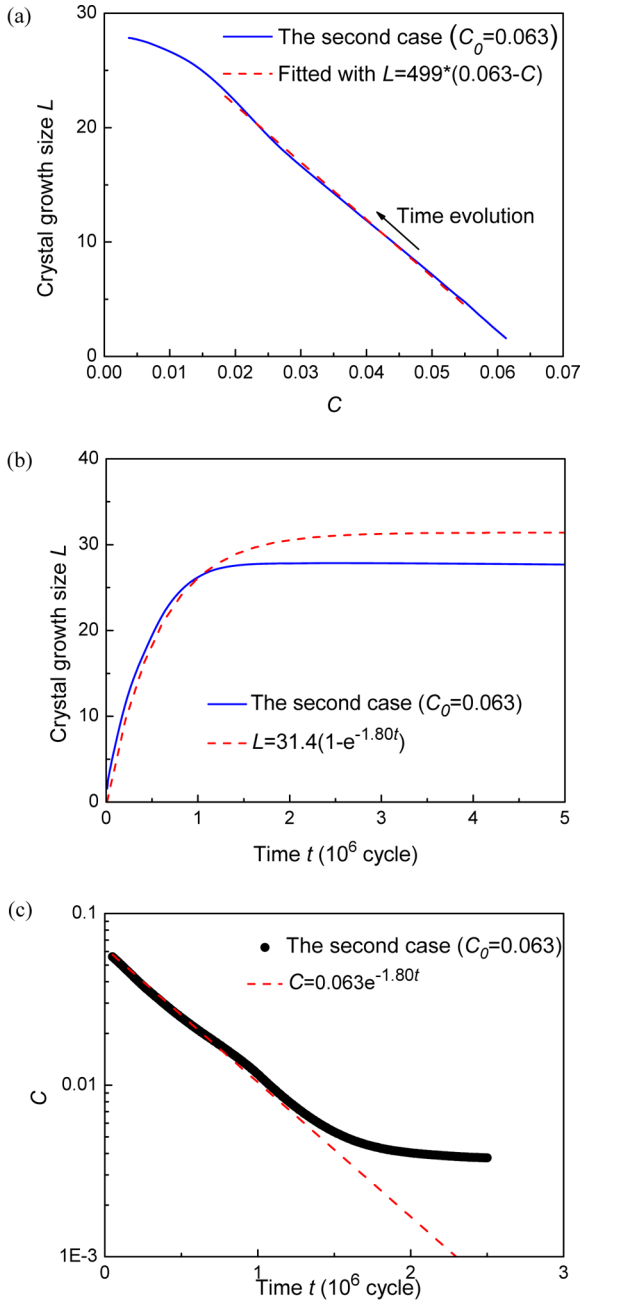

Figure 8. Comparison of the fitting theoretical curves with the simulation results for the second case with the chain length $N = 64$, the temperature $T = 3.4$, and the initial concentration $C_0 = 0.063$: (a) the linear crystal growth sizes versus polymer volume fractions; (b) the linear crystal growth sizes versus time evolution; (c) polymer volume fractions versus time evolution.

IV. CONCLUSION

Dynamic Monte Carlo simulations of quasi-1D lamellar crystal growth in polymer solutions demonstrated a linear relationship between linear crystal growth rates and polymer concentrations, which characterizes the surface-nucleation-controlled mechanism of crystal growth with either constant or decaying polymer concentrations. On the basis of this linear relationship, the exponential-decay function can be applied to treat the time evolution of quasi-1D crystal growth sizes in the case of massive crystals growing in the limited size of polymer solutions, which

dx.doi.org/10.1021/jp311889n | J. Phys. Chem. B 2013, 117, 3047−3053

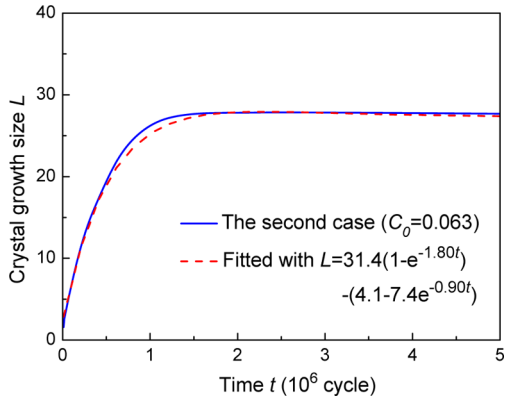

Figure 9. Comparison between the time-evolution curve of linear crystal growth sizes in Figure 8b and the double-exponential fitting with the fixed parameters in the first exponential term. The second case contains the chain length N = 64, the temperature T = 3.4, and the initial concentration C_0 = 0.063.

provides a theoretical model to the data analysis of the corresponding experimental systems.

AUTHOR INFORMATION

Corresponding Author

*E-mail: wbhu@nju.edu.cn. Phone: 86-25-83596667.

Notes

The authors declare no competing financial interest.

ACKNOWLEDGMENTS

We appreciated the very stimulating and helpful communications with Prof. Mitchell A. Winnik, Dr. Jieshu Qian, and Dr. Gerald Guerin at Department of Chemistry, University of Toronto. The work was supported by National Natural Science Foundation of China (Grant Nos. 20825415 and 21274061) and the National Basic Research Program of China (Grant No. 2011CB606100).

REFERENCES

(1) Bennett, R. C. Crystallization from Solution. In *Chemical Engineers' Handbook*; McGraw-Hill: New York, 1984; pp 19.24−19.40.
(2) Myerson, A. S. *Handbook of Industrial Crystallization*, 2nd ed.; Butterworth-Heinemann: Boston, MA, 2002.
(3) Wunderlich, B. *Macromolecular Physics*; Academic Press: New York, 1976; Vol. 2.
(4) Keller, A. A Note on Single Crystals in Polymers: Evidence for a Folded Chain Configuration. *Philos. Mag.* **1957**, *2*, 1171−1175.
(5) Lauritzen, J. I.; Hoffman, J. D. Theory of Formation of Polymer Crystals with Folded Chains in Dilute. Solution. *J. Res. Natl. Bur. Stand., Sect. A* **1960**, *64*, 73−102.
(6) Sanchez, I. C.; Dimarzio, E. A. Dilute Solution Theory of Polymer Crystal Growth: A Kinetic Theory of Chain Folding. *J. Chem. Phys.* **1971**, *55*, 893−908.
(7) Point, J. J.; Colet, M. C.; Dosiere, M. Experimental Criterion for the Crystallization Regime in Polymer Crystals Grown from Dilute Solution: Possible Limitation due to Fractionation. *J. Polym. Sci., Polym. Phys.* **1986**, *24*, 357−388.
(8) Armistead, K.; Goldbeckwood, G.; Keller, A. Polymer Crystallization Theories. *Adv. Polym. Sci.* **1992**, *100*, 221−312.
(9) Welch, P.; Muthukumar, M. Molecular Mechanisms of Polymer Crystallization from Solution. *Phys. Rev. Lett.* **2001**, *87*, 218302(1)−218302(4).
(10) Hu, W. B.; Cai, T. Regime Transitions of Polymer Crystal Growth Rates: Molecular Simulations and Interpretation beyond Lauritzen-Hoffman Model. *Macromolecules* **2008**, *41*, 2049−2061.
(11) Gädt, T.; Ieong, N. S.; Cambridge, G.; Winnik, M. A.; Manners, I. Complex and Hierarchical Micelle Architectures from Diblock Copolymers using Living, Crystallization-Driven Polymerizations. *Nat. Mater.* **2009**, *8*, 144−150.
(12) Qian, J. S.; Guerin, G.; Lu, Y. J.; Cambridge, G.; Manners, I.; Winnik, M. A. Self-Seeding in One Dimension: An Approach To Control the Length of Fiberlike Polyisoprene−Polyferrocenylsilane Block Copolymer Micelles. *Angew. Chem., Int. Ed.* **2011**, *50*, 1622−1625.
(13) Keller, A.; Pedemonte, E. A Study of Growth Rates of Polyethylene Single Crystals. *J. Cryst. Growth* **1973**, *18*, 111−123.
(14) Cooper, M.; Manley, R. S. J. Growth Kinetics of Polyethylene Single Crystals. I. Growth of (110) Faces of Crystals from Dilute Solutions in Xylene. *Macromolecules* **1975**, *8*, 219−227.
(15) Toda, A. Growth Kinetics of Polyethylene Single Crystals from Dilute Solution at Low Supercoolings. *Polymer* **1987**, *28*, 1645−1651.
(16) Ding, N.; Amis, E. J. Kinetics of Poly(ethylene oxide) Crystallization from Solution: Concentration Dependence. *Macromolecules* **1991**, *24*, 6464−6469.
(17) Toda, A.; Kiho, H. Crystal Growth of Polyethylene from Dilute Solution: Growth Kinetics of {110} Twins and Diffusion-Limited Growth of Single Crystals. *J. Polym. Sci., Part B: Polym. Phys.* **1989**, *27*, 53−70.
(18) Sadler, D. M. New Explanation for Chain Folding in Polymers. *Nature* **1987**, *326*, 174−177.
(19) Ren, Y. J.; Ma, A. Q.; Li, J.; Jiang, X. M.; Ma, Y.; Toda, A.; Hu, W.-B. Melting of Polymer Single Crystals Studied by Dynamic Monte Carlo Simulations. *Eur. Phys. J. E* **2010**, *33*, 189−202.
(20) Yamamoto, T. Computer Modeling of Polymer Crystallization − Toward Computer-Assisted Materials' Design. *Polymer* **2009**, *50*, 1975−1985.
(21) Chen, C.-M.; Higgs, P. G. Monte-Carlo Simulation of Polymer Crystallisation in Dilute Solution. *J. Chem. Phys.* **1998**, *108*, 4305−4314.
(22) Zhang, J.; Muthukumar, M. Monte Carlo Simulations of Single Crystals from Polymer Solutions. *J. Chem. Phys.* **2007**, *126*, 234904(1)−234904(18).
(23) Hu, W. B.; Frenkel, D. Polymer Crystallization Driven by Anisotropic Interactions. *Adv. Polym. Sci.* **2005**, *191*, 1−35.
(24) Hu, W. B. Intramolecular Crystal Nucleation. *Lect. Notes Phys.* **2007**, *714*, 47−63.
(25) Cai, T.; Ma, Y.; Yin, P.-C.; Hu, W.-B. Understanding the Growth Rates of Polymer Co-crystallization in the Binary Mixtures of Different Chain Lengths. *J. Phys. Chem. B* **2008**, *112*, 7370−7376.
(26) Qian, J. S.; Lu, Y. J.; Cambridge, G.; Guerin, G.; Manners, I.; Winnik, M. A. Growth Kinetics and Mechanism for the Crystallization-Driven Self-Assembly of One-Dimensional Poly(isoprene-b-ferrocenyldimethylsilane) Block Copolymer Micelles. Manuscript to be submitted.